Brain Pathology 8: 487-498 (1998)

RESEARCH ARTICLE

Microvascular and Cellular Responses in the Retina of Rats with Acute Experimental Allergic Encephalomyelitis (EAE)

Ping Hu[1], John Pollard[2], Nicholas Hunt[3], Tailoi Chan-Ling[1]

[1] Department of Anatomy and Histology, Institute of Biomedical Research, [2]Department of Medicine, and [3]Department of Pathology, University of Sydney, Sydney NSW 2006, Australia

The microvascular and cellular responses in the retina during acute EAE were characterized using whole-mount preparations. The earliest detectable event was the accumulation of monocytes and T cells within veins on day 7 postinduction (pi). Mild breakdown of the blood-retinal barrier (BRB), activation of microglia and infiltration of monocytes and T cells into the retinal parenchyma were first evident on days 7 to 8 pi. Monocyte adhesion to the vessel wall and breakdown of the BRB were colocalized in the same vessel segments and occurred predominantly in veins. The marked difference in response observed in the retina versus the myelinated region of the optic nerve suggests that two types of inflammatory cascades are initiated. A mild response, characterised by very low numbers of T cells and monocytes and an absence of expression of MHC class II by resident microglia, is initiated when only small amounts of the encephalitogenic antigen are present in the perivascular space or associated with perivascular antigen-presenting cells. A full blown inflammatory reaction, as observed in the optic nerve, is initiated in the presence of substantial amounts of encephalitogenic antigen. This severe response is characterised by the infiltration of large numbers of $CD4^+$, $CD8^+$ T cells and $ED1^+$ monocytes, and by abundant MHC class II expression by resident microglia as well as other cell types. Thus, MHC class II expression by resident microglia may be a possible effective amplifier mechanism if the encephalitogenic antigen is encountered in the tissue parenchyma.

Corresponding Author:
Dr. Tailoi Chan-Ling, Department of Anatomy and Histology F13, University of Sydney, Sydney NSW 2006, Australia;
Tel.: 61 2 9351 2596; Fax: 61 2 9351 6556;
E-mail: tailoi@anatomy.usyd.edu.au

Introduction

Whole-mount preparations of the retina offer unique advantages for studying the pathogenesis of EAE, especially the role of breakdown of the blood-brain barrier (BBB) (Chan-Ling *et al*., 1992). EAE is a T cell-mediated, autoimmune demyelinating disease of the central nervous system (CNS) and serves as an animal model of multiple sclerosis (MS). In both EAE and MS, the early CNS lesions are characterized by increased vascular permeability, cellular infiltration, and local glial responses (Hickey, 1991; Wekerle, 1993). These changes have been studied predominantly in spinal cord and brain tissue, although microvascular and cellular responses have also been described in the retina in both EAE (Sallmann *et al*., 1967; Rao *et al*., 1977; Hayreh, 1981) and MS (Arnold *et al*., 1984; Engell *et al*., 1985; Lightman *et al*., 1987). The retina, being an outgrowth of the diencephalon embryologically, is representative of microvascular and cellular changes in other regions of the CNS (reviewed in Chan-Ling, 1994). Perivascular tracer leakage and cellular infiltration in a nonmyelinated tissue such as the retina have suggested to some workers that vascular changes in MS can occur independently of demyelination and may be the primary event in the formation of new lesions (Lightman *et al*., 1987; Wray, 1997).

Despite some reports of retinal involvement in animal models of EAE, a large number of studies have failed to detect T cell infiltration in the retina (Hayreh, 1981; Sallmann *et al*., 1967; Shikishima *et al*., 1993; Verhagen *et al*., 1994). Because of these conflicting results, and to increase our understanding of the mechanisms that underlie initiation of EAE lesions, we have now examined the localization, time courses, and relationships among breakdown of the BRB, cellular infiltration and microglial activation in whole-mount preparations of retinas from Lewis rats with MBP-induced EAE.

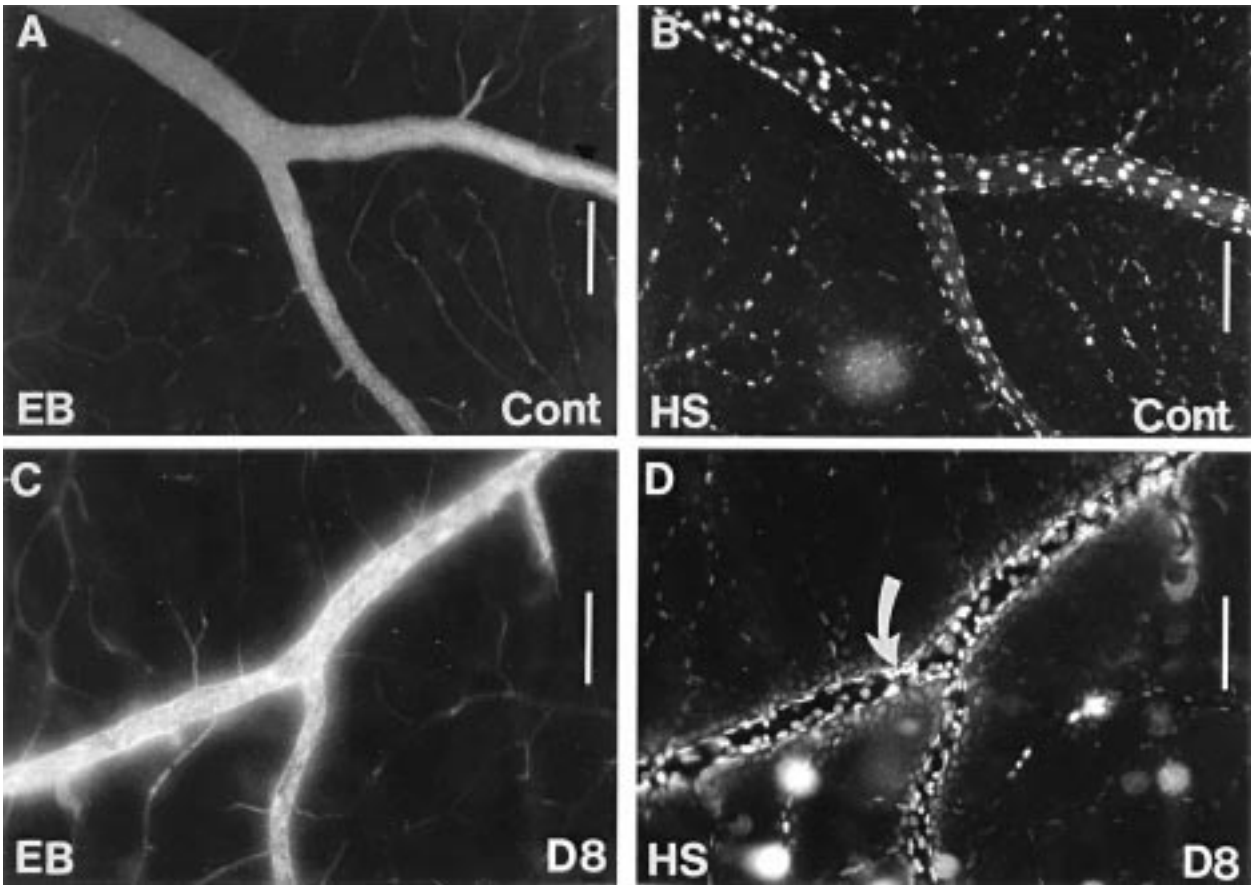

Figure 1. Relation between vessel leakage and inflammatory cells in EAE retinae. (**A**) A naive rat: no leakage of Evans blue (EB); blood vessels showed sharp outlines. (**B**) Nuclei of vascular endothelial cells in the same blood vessels as (**A**) shown by Hoechst stain (HS); these cells showed a rounded morphology typical of veins and were distributed evenly along the vessels. A few nucleated cells were also present in the vessels. (**C**) Rat with EAE day 8 pi. EB leakage producing blurred vessel outline. (**D**) Accumulation of non-endothelial HS-labeled cells (curved arrow) in the leaky segment of the same blood vessels as (**C**). BRB breakdown evident as a rim of bis-benzimide-stained somata in the perivascular region. Scale bars, 50 μm.

Materials and Methods

Experimental animals and tissue preparation. *Animals*: Acute EAE was induced in 120 male JC Lewis rats by intradermal injection of purified MBP and examined at various times as detailed in the preceding manuscript. Experimental animals were compared with a total of 40 naive control rats as well as animals inoculated with Freund's adjuvant containing M. tuberculosis alone.

Retinal whole-mount preparations: The eyes were enucleated, and the anterior segment, crystalline lens, and vitreous were removed while the eyes were floating in PBS (Chan-Ling, 1997). For detection of HRP, the trichrome technique, and GS lectin histochemistry, the eyecup was fixed by immersion for 30 min in PBS containing 4% (w/v) paraformaldehyde. For ED1, MHC class II antigen, and TCR immunohistochemistry, dissection of the retina was completed in PBS before immersion fixation for 20 min in acetone (-20°C).

Preparation of retinal sections: The eyecup was fixed by immersion in PBS containing 2.5% (v/v) glutaraldehyde, embedded in resin, sectioned at 0.25 μm, and stained with toluidine blue (Pollard *et al*., 1995).

Identification of microvascular responses. *Horseradish peroxidase (HRP) and Monastral blue*: HRP and Monastral blue administration were as detailed in the preceding manuscript. Retinal wholemounts were then placed onto a slide coated with 8% (w/v) gelatin, dried in air, dehydrated, cleared and mounted.

Trichrome technique: The tail vein of rats was injected with 0.5 ml of 4% (w/v) Evans blue (Sigma) dissolved in saline and 0.5 ml of 1% (w/v) bis-benzimide

Time (days pi)	n	ED1+ cells/ mm2			TCR+ cells/ mm2		MHC class II+ cells/ mm2	
		Intravascular	Parenchymal					
			Microglial-like	Monocyte-like	Intravascular	Parenchymal	Intravascular	Parenchymal
Naive Control	3	0.20 ± 0.28	0.0 ± 0.0	0.0 ± 0.0	0.15 ± 0.21	0.0 ± 0.0	0.0 ± 0.0	0.0 ± 0.0
Inoculated Control	6	0.37 ± 0.47	0.02 ± 0.04	0.0 ± 0.0	0.22 ± 0.22	0.02 ± 0.04	0.0 ± 0.0	0.0 ± 0.0
7 to 8	7	5.1 ± 4.5 (p = 0.017)*	1.91 ± 3.81 (p = 0.212)	0.59 ± 1.3 (p = 0.241)	2.17 ± 2.69 (p = 0.081)	0.2± 0.25 (p = 0.071)	6.03 ±1.22 (p = 0.024)*	0.07 ± 1.3 (p = 0.156)
10 to 12	7	2.3 ± 1.9 (p = 0.022)*	2.06 ± 3.79 (p = 0.18)	0.61 ± 1.17 (p = 0.19)	1.34 ± 1.28 (p = 0.043)*	0.7 ± 0.82 (p = 0.048)*	0.79 ± 1.05 (p = 0.069)	0.14 ± 0.18 (p = 0.074)
14 to 17 ± 0.22	7	4.8 ± 9.5 (p = 0.242)	0.54± 0.74 (p = 0.83)	0.3 ± 0.37 (p = 0.053)	0.98 ± 1.55 (p = 0.23)	0.36 ± 0.34 (p = 0.02)*	0.31 ± 0.5 (p = 0.12)	0.14 (p = 0.122)
20 to 28	4	3.08 ± 3.19 (p = 0.047)*	11.5 ± 10.84 (p = 0.017)*	1.19 ± 1.12 (p = 0.017)*	3.85 ± 4.37 (p = 0.048)*	6.88 ± 6.71 (p = 0.02)*	0.0 ± 0.0	0.0 ± 0.0

Data are means ± SD. * Statistically significant difference vs. control (student's t-test).

Table 1. Density of ED1+ , TCR+, and MHC class II+ cells in the retinal vessels and parenchyma of JC Lewis rats during progression of acute EAE.

dissolved in saline (Chan-Ling *et al*., 1992). Both solutions were passed through a nonpyrogenic sterile 0.22-μm filter (Millipore, Bedford, USA) immediately before injection. The animals were killed 10 min after injection of tracers. The injection of both Evans blue (Fig 1A, C) and bis-benzimide (Fig 1B, D) allows the colocalization of sites of barrier breakdown and cellular infiltration. The third element of the trichrome technique, red blood cells within the lumen of vessels, is detected by transmitted light microscopy, providing additional information on rheology.

Detection of the αβTCR, ED1 and MHC class II antigen and GS lectin histochemistry.

Retinal wholemounts were reacted while freely floating in solution and all procedures were done on a gently rocking surface to facilitate tissue penetration. All procedures followed were as detailed in the preceding manuscript with the exception that retinae were washed for 30 minutes between incubations and incubation times for primary and secondary antibodies were overnight and two hours respectively. HRP-conjugated *Griffonia simplicifolia* isolectin B4 was used to label microglia and monocytes and the retina processed as detailed previously (Chan-Ling *et al*., 1990).

Quantitative cellular analysis. The time course of the appearance of each cell type within the vessel lumen as well as the time course of cellular extravasation were quantified separately. Cells were considered positive for TCR, the ED1 antigen, or MHC class II if they exhibited dense, dark brown immunoreactivity. ED1+ cells frequently exhibited Monastral blue particles as well as cytoplasmic inclusions. Cells were counted with either a 20X or 40X objective, and a mean density was calculated for each time point. Data are presented as means ± SD and were analyzed by Student's t test or chi-square test as indicated. A *P* value of <0.05 was considered statistically significant.

Time (days pi)	Leakage (EAE)		Leakage (Inoculated Control)	
	Evans blue	HRP	Evans blue	HRP
7	0, 0, 1	0, 1, 0	0	0
8	1, 1, 3*	1, 1, 2*	0	0
10	1, 1, 3*	1, 3, 3*	0	0
12	1, 2, 3*	1, 1, 4*	0	0
14	1, 1, 4*	2, 2, 4*	0	0
17	1, 1, 3*	1, 3, 3*	0	0
28	0, 1, 2	1, 1, 2*	0	0

Grades refer to individual animals and are as follows: 0, equivalent to the level of tracer leakage apparent in control rats; 1, one to three sites of mild tracer leakage; 2, more than three sites of mild tracer leakage or one to three sites of medium leakage; 3, more than three sites of medium leakage or one to three sites of severe leakage; 4, more than three sites of severe leakage.
* $p < 0.05$ vs. control (chi square test).

Table 2. Subjective microscopic grading of Evans blue and HRP leakage from retinal vessels in rats with acute EAE from days 7 to 28 pi.

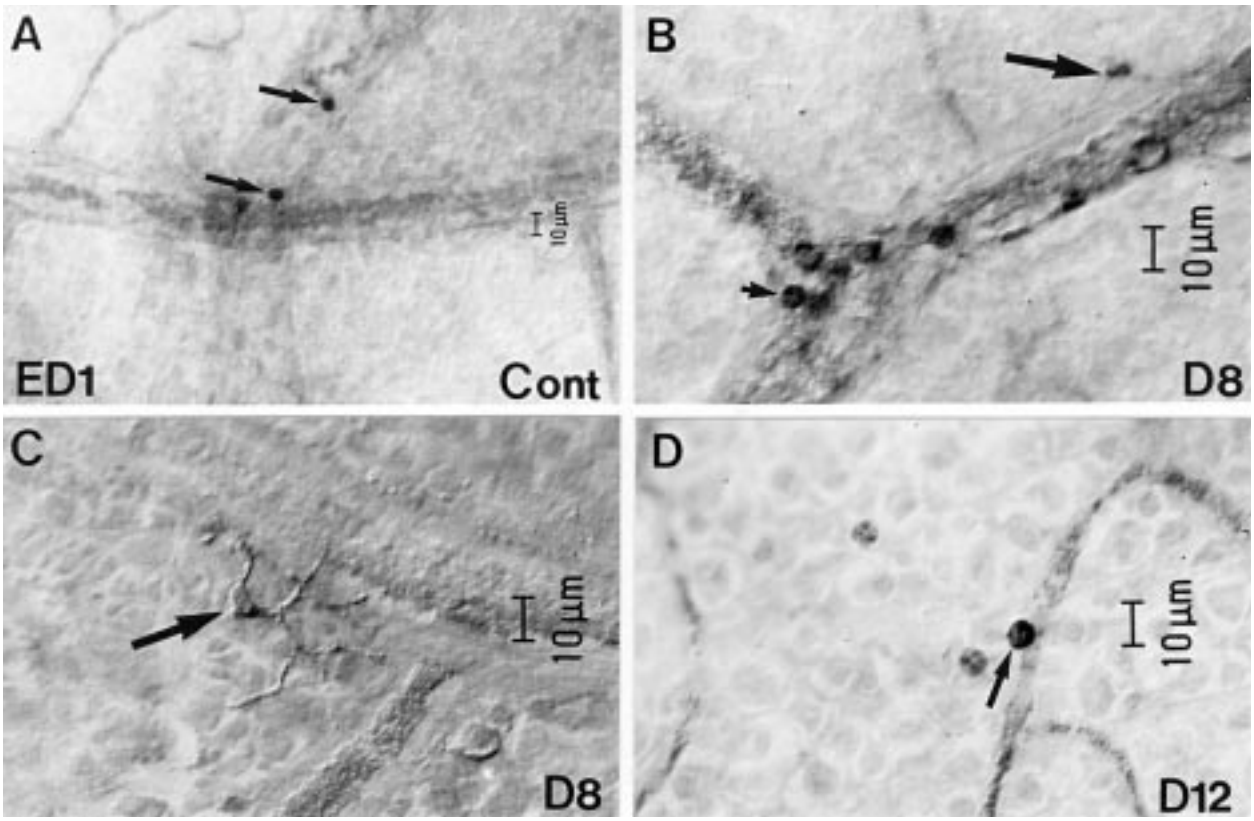

Figure 2. ED1$^+$ monocytes and microglia in EAE retinae. (**A**) Naive control rat: two ED1$^+$ monocytes in a vein in central retina (arrows). (**B**) EAE, day 8 pi: several ED1$^+$ monocytes (small arrow) at branch point of a vein in peripheral retina. One ED1$^+$ microglial cell with fine processes evident in the perivascular parenchyma (large arrow). (**C**) Arrow indicates a ramified ED1$^+$ microglial cell at the vessel branch point. (**D**) Three ED1$^+$ cells in the parenchyma at day 12 pi; one contains Monastral blue particles within its cytoplasm (arrow), suggestive of phagocytic activity.

Results

Trafficking of leukocytes within normal CNS vessels. The mean density of ED1$^+$ and TCR$^+$ cells within the lumen of vessels in naive control animals was 0.20 ± 0.28 cells/mm^2 and 0.15 ± 0.21 cells/mm^2 respectively (Table 1). The low numbers and discrete location of ED1$^+$ and αβTCR$^+$ cells within the lumen of retinal vessels, together with their apparent lack of adhesion to the vessel wall (Fig. 2A), suggest that their presence reflects normal trafficking through CNS vessels. No MHC class II$^+$ cells were detected within the vessels or parenchyma of any control animals (Table 1).

Absence of cellular and microvascular response in inoculated control animals. Intravascular injection of HRP (Fig. 3A) and Evan's Blue (Table 2) revealed no evidence of breakdown of the BRB in inoculated control animals throughout the observation period. Following application of cell-specific markers as detailed above, no increase in cellular response, above that detected in naive control animals, was observed in the retina of inoculated control rats throughout the observation period.

Figure 3. (Opposing page) Time course of HRP leakage from inner retinal vessels of rats with EAE as revealed by retinal whole-mount preparations. (**A**) Inoculated control rats: no extravasation of tracer. Vessels well perfused with plasma and showed sharp outlines. (**B**) Focal regions of a mild BRB breakdown first evident at day 7 pi. (**C**) Day 8 pi: Leakage shown by HRP accumulation in the perivascular region causing blurring of vessel outline. (**D-E**) Extensive HRP leakage at branch points of veins, days 10 to 12 pi. Tracer leakage was evident from one or several veins. (**F**) Leakage of HRP from retinal vessels was greatest at day 14 pi. Little HRP is retained within the vessel lumen and is mostly trapped in the perivenous region. (**G**) Significant leakage of HRP still evident at day 17 pi. (**H**) A low level of HRP leakage apparent at branch points of some veins at day 28 pi.

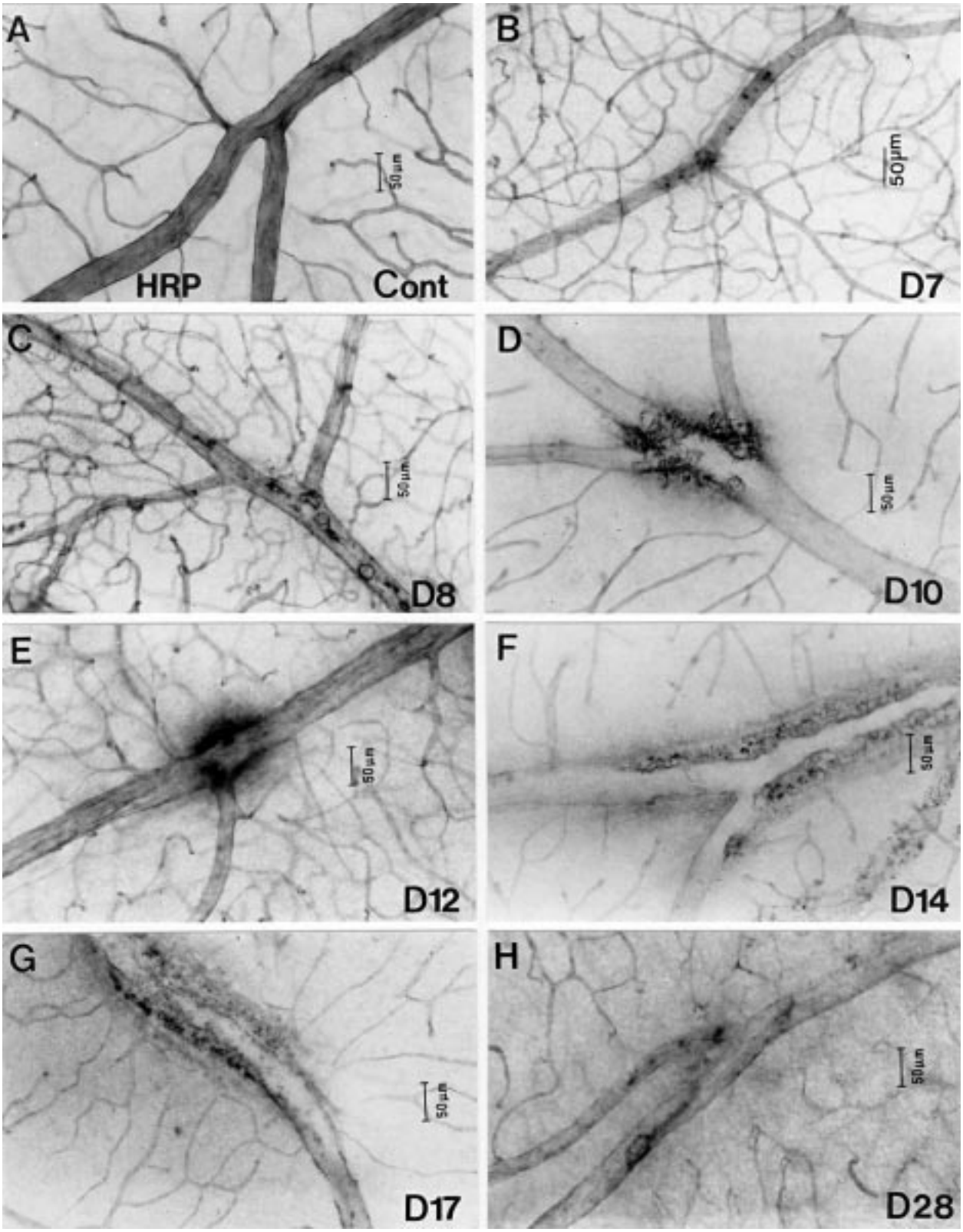
A
HRP
Cont
50 µm
B
D7
50µm
C
D8
50µm
D
D10
50µm
E
D12
50µm
F
D14
50µm
G
D17
50µm
H
D28
50µm

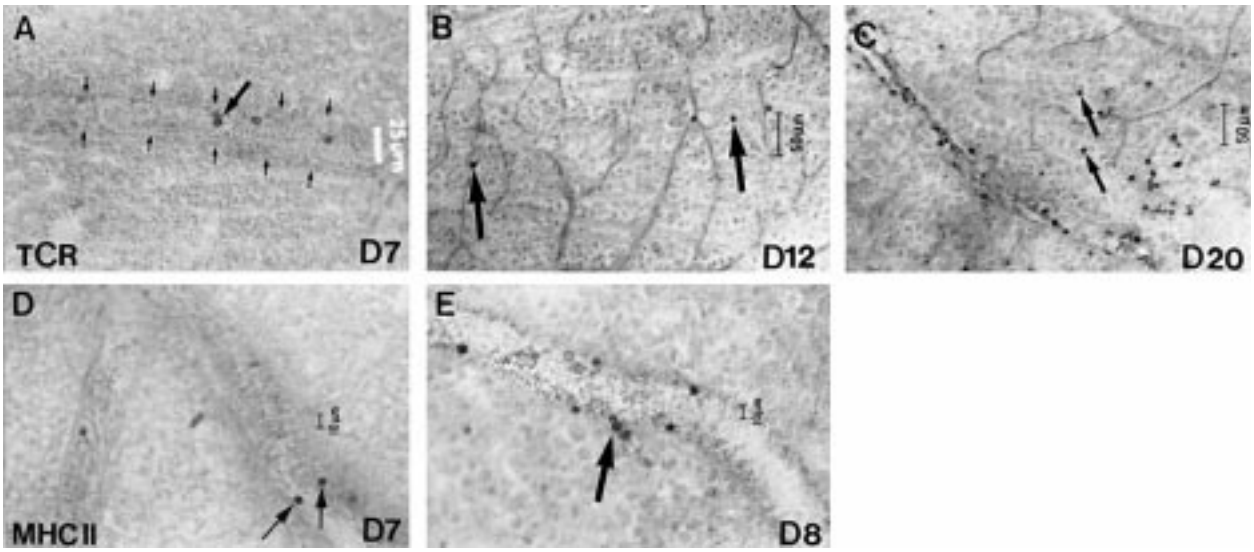

Figure 4. TCR$^+$ and MHC class II$^+$ cells in retinae of rats with EAE. (**A**) TCR$^+$ cells (large arrow) within the lumen of a vein at day 7 pi, small arrows indicate the border of the blood vessel. (**B**) TCR$^+$ cells in retinal parenchyma at day 12 pi (arrows). (**C**) TCR$^+$ cells in vessels and parenchyma of the retina at day 20 pi (arrows). (**D**) MHC class II$^+$ cells in a vein within central retina at day 7 pi (arrows). (**E**) Increased numbers of MHC class II$^+$ cells at day 8 pi. Some cells were within the lumen of the vessel while some had just extravasated (arrow).

Cellular cascade and breakdown of the BRB during acute EAE. *Adhesion of αβTCR$^+$ T cells and ED1$^+$, MHC class II$^+$ monocytes within retinal veins from day 7 pi*: On day 7 pi, increased numbers of TCR$^+$ (Fig. 4A, Table 1) and ED1$^+$ cells (Table 1) were evident predominantly within the lumen of retinal veins. MHC class II$^+$ monocytes/macrophages were also evident within retinal veins on day 7 pi (Fig. 4D); these cells aggregated in the region adjacent to the vessel wall. Table 1 shows the density of ED1$^+$, TCR$^+$, and MHC class II$^+$ cells within the lumen of the retinal blood vessels and parenchyma during EAE. The average density of intravascular ED1$^+$, TCR$^+$, or MHC class II$^+$ cells on day 7 pi was 4.1 ± 3.9, 4.5 ± 4.5, and 4.8 ± 5.8 cells/mm^2, respectively. Figure 2B show significant numbers of ED1$^+$ monocytes/macrophages accumulating within the lumen of retinal veins at day 8 pi.

First breakdown of the BRB at day 7 to 8 pi: Figure 3 shows the changes in retinal barrier properties during the course of EAE as demonstrated by intravascular perfusion of HRP. On day 7 pi, a mild breakdown of the BRB was apparent in a small proportion of rats (Fig. 3B). The first consistently detectable increase in permeability to HRP, albeit small, was evident on day 8 pi (Fig. 3C). On days 10 to 12 pi, an increase in leakage of HRP was evident in focal regions across the retina (Fig. 3, D and E). Vascular permeability was maximal on day 14 pi (Fig. 3F). The extent of tracer leakage decreased from day 17 pi (Fig. 3G), but was still apparent at a low level on day 28 pi (Fig. 3H). Intravascular injection of Evans blue revealed a similar change in barrier properties during the course of EAE (Table 2). There was a substantial amount of variability among animals at each time point. In contrast to the optic nerve, even at the period of peak HRP and Evans blue leakage, no leakage of Monastral blue from retinal vessels was evident.

Activation of microglia from day 7 to 8 pi: Microglia stained only weakly with GS lectin in the retina of both naive and inoculated control animals (Fig. 5, A and G). From days 7 to 8 pi, GS lectin$^+$ microglia in the retina

Figure 5. (Opposing page) Microglial activation as revealed by GS lectin histochemistry. (**A**) In inoculated control rats, microglia exhibited a ramified morphology. (**B**) At day 7 pi, microglial processes have become shorter and somata larger as they assume a rod-shape. (**C**) At day 8 pi, rod-shaped microglia characterized by irregular, swollen soma and pseudopodia with focal regions of increased GS lectin reactivity. (**D**) Significant variation in the morphology of GS lectin$^+$ cells at day 10 pi: one GS lectin$^+$ cell (small arrow) with an irregular morphology with small vacuoles, another (large arrow) exhibits a ramified morphology with many distensions along the processes. (**E**) GS lectin$^+$ cells with ramified morphology and distensions along the processes apparent at day 12 pi. (**F**) Many monocyte-like GS lectin$^+$ cells within a vein at day 14 pi; some cells appear to be in the process of extravasation (arrows). (**G**) Ramified microglia in naive control rats were evenly distributed. (**H**) At day 8 pi, GS lectin$^+$ ramified microglia had redistributed to the perivascular region.

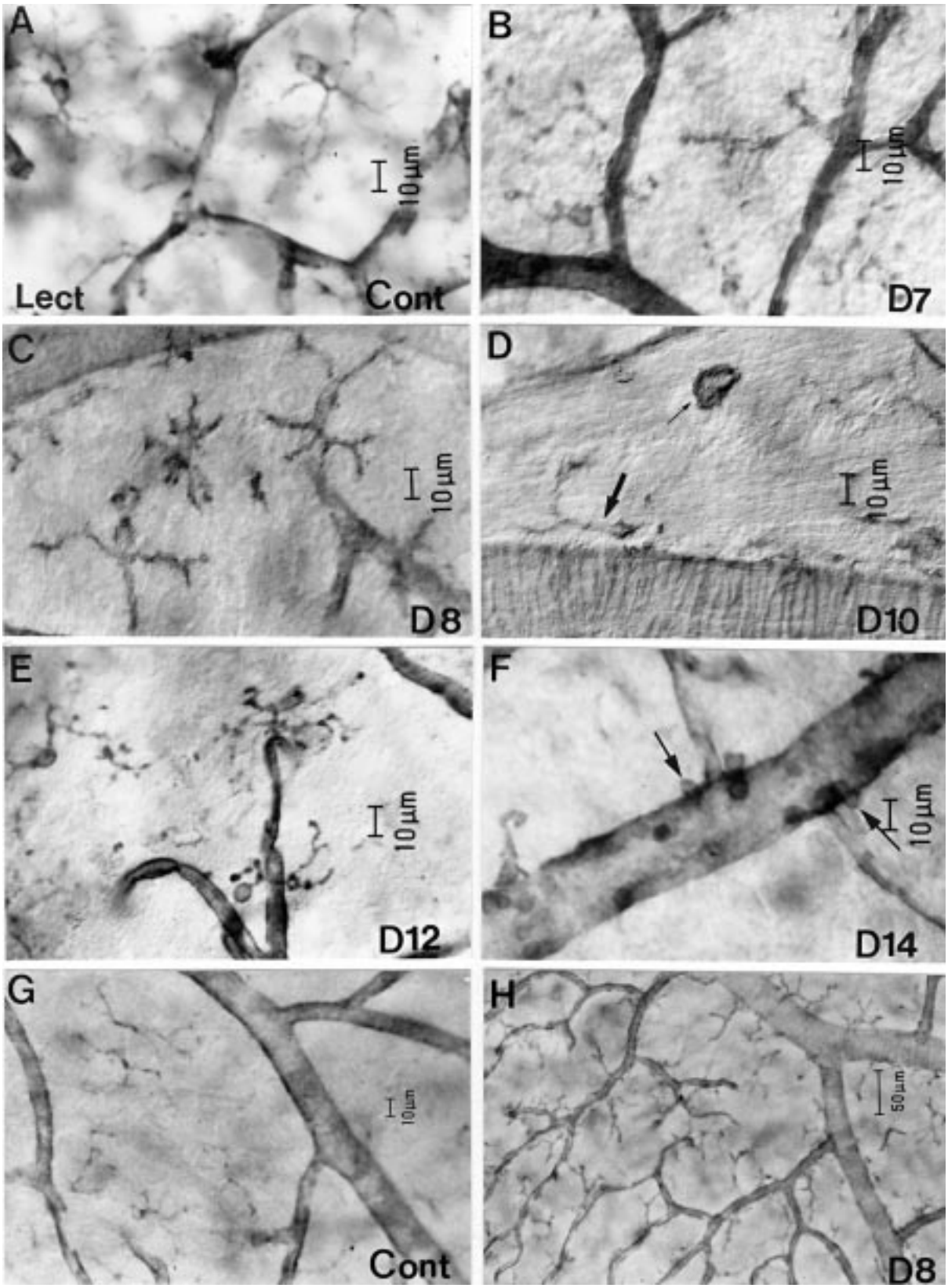
A
10µm
Lect
Cont
B
10µm
D7
C
10µm
D8
D
10µm
D10
E
10µm
D12
F
10µm
D14
G
10µm
Cont
H
50µm
D8

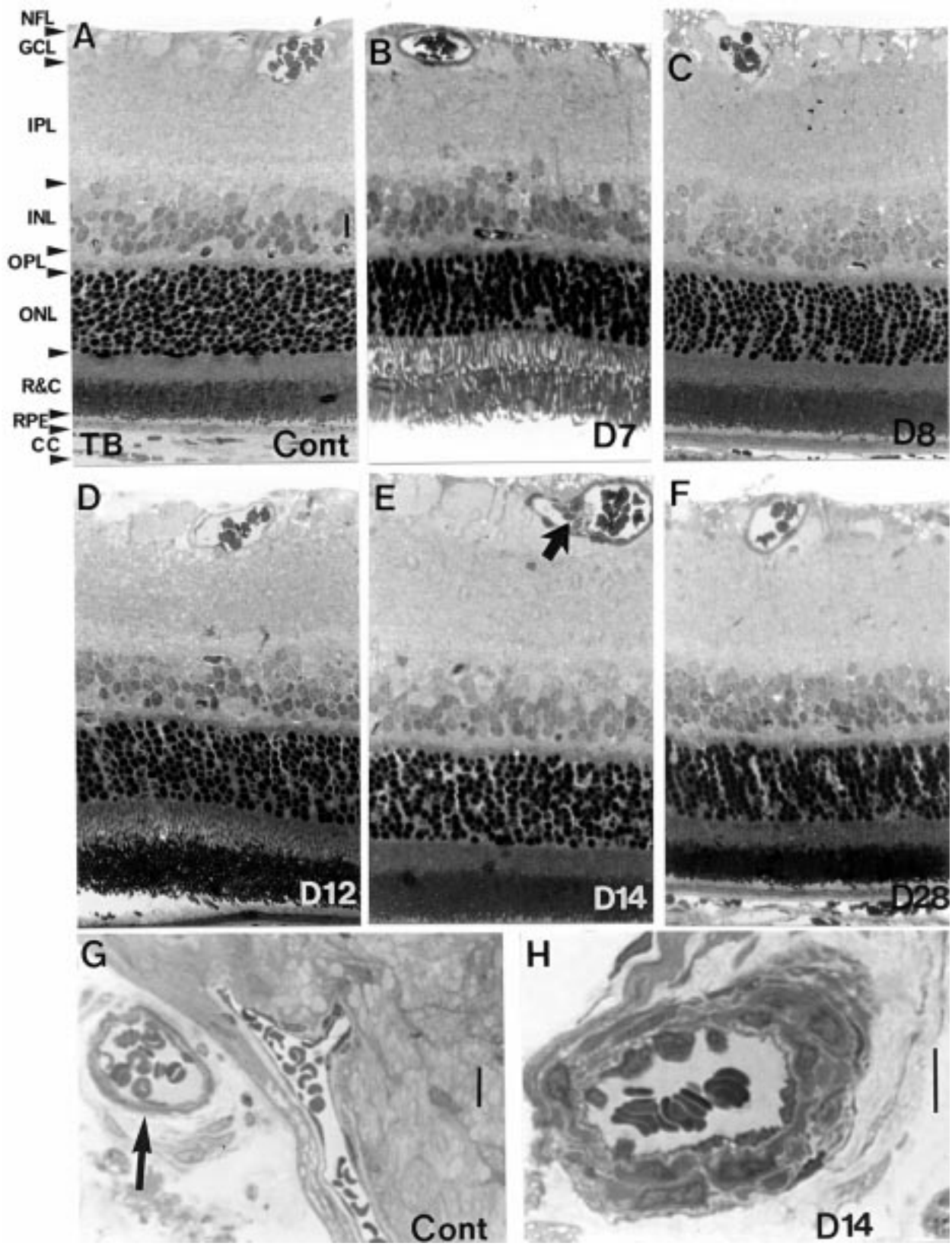
NFL
GCL
IPL
INL
OPL
ONL
R&C
RPE
CC
A
TB
Cont
B
D7
C
D8
D
D12
E
D14
F
D28
G
Cont
H
D14

adopted an amoeboid morphology and increased in numbers (Fig. 5 B and C). From days 10 to 12 pi, three types of GS lectin$^+$ cells were apparent in focal regions of the parenchyma: (i) ramified cells with distensions along their processes (Fig. 5, D and E), (ii) rod-shaped cells, and (iii) cells without processes, which were 10 to 14 μm in diameter and of irregular morphology, and some of which contained small vacuoles or GS lectin$^+$ granules (Fig. 5D). However, cells with processes constituted the largest GS lectin$^+$ population (Fig. 5, D and E). On days 14 to 17 pi, the number of GS lectin$^+$ cells had decreased markedly. Most showed a ramified form, although a few were rod-shaped. Some GS lectin$^+$ monocytes were also apparent in the perivascular parenchyma (Fig. 5F). On day 28 pi, nearly all the GS lectin$^+$ cells in the parenchyma showed a ramified morphology.

A few ED1$^+$ cells with a morphology typical of microglia were detected in the parenchyma surrounding blood vessels on days 8 pi (Fig. 2B & C), and 10 pi, increasing significantly in number at days 20 pi and 28 pi.

Association of sites of focal vessel leakage with leukocyte accumulation: With the trichrome technique, we demonstrated that the sites of focal leakage from retinal vessels were coincident with sites of leukocyte accumulation. Figure 1C shows leakage of Evans blue from a segment of a retinal vein from an EAE rat on day 8 pi, and Fig. 1D shows the accumulation of bis-benzimide-labeled leukocytes in this same venous segment. Incubation of this same tissue with HRP-conjugated GS lectin revealed that the site of leukocyte accumulation was associated with GS lectin$^+$ monocytes.

Association of BRB breakdown with redistribution of microglia toward blood vessels: In control animals, most microglia are not closely associated with retinal blood vessels; rather, they are distributed regularly within the parenchyma (Fig. 5A & G). From day 8 pi, microglia in the retina of EAE rats tended to congregate around blood vessels (Fig. 5H), both arteries and veins. This redistribution was apparent throughout the retina in association with a low-level diffuse breakdown of the BRB.

Evidence of extracellular edema, leukocyte accumulation, and a perivascular cell response from retinal sections beginning on days 7 to 8 pi: In control rats, red blood cells were evident in the lumen of the inner retinal vascular plexus and few extracellular spaces were apparent throughout the retinal layers (Fig. 6A). From day 7 pi, mild edema was detected in the nerve fiber layer of the retina in a small proportion of EAE animals and the contents of the vascular lumen appeared clumped (Fig. 6B). From days 7 to 17 pi, perivascular cells appeared enlarged (Fig 6B-E, H). The extent of extracellular edema was increased on day 8 (Fig. 6C), peaked on days 12 (Fig. 6D) and 14 (Fig. 6E), and became mild again by day 28 pi (Fig. 6F). Accumulation of mononuclear cells was observed from days 8 to 28 pi (Fig. 6E). These changes were evident only in the inner retinal vascular plexus and the surrounding parenchyma.

Extravasation of TCR$^+$ lymphocytes and monocytes labeled with GS lectin, ED1, or OX6 from the postcapillary vasculature from day 8 pi: Small numbers of TCR$^+$ lymphocytes and ED1$^+$ or MHC class II$^+$ monocytes had extravasated and were first evident within the parenchyma from day 8 pi. When the density of ED1$^+$ microglia (with distinct processes) and ED1$^+$ monocytes/macrophages (round soma with no processes) were determined individually, ED1$^+$ microglia had a mean density of 3.3 ± 2.4 cells/mm^2 , while ED1$^+$ monocytes/macrophages had a mean density of 1.0 ± 0.8 cells/mm^2. On day 8 pi, the mean density of MHC class II$^+$ monocytes in the parenchyma was only 0.2 ± 0.2 cells/mm^2, while the mean density of TCR$^+$ lymphocytes was 0.3 ± 0.3 cells/mm^2. Most ED1$^+$ monocytes or microglia (Fig. 2B, C) and MHC class II$^+$ monocytes detected in the parenchyma were located in close proximity to either a vein, venule, or postcapillary venule (Fig. 4E). Figure 5F shows several GS lectin$^+$ monocytes possibly in the process of diapedesis from a vein. From these observations, we conclude that monocytes predominantly extravasate from the venous vasculature during acute EAE.

From day 12 pi onwards, the number of TCR$^+$ lymphocytes (Figs. 4B & C) and ED1$^+$ cells (Fig 2D, Table 1) within the parenchyma increased significantly. Unlike the ED1$^+$ or MHC class II$^+$ cells, which were

Figure 6. Retinal histology during EAE. (**A**) The normal structure of the retina in inoculated control animals. (**B**) Mild edema in nerve fiber layer at day 7 pi. (**C-D**) Extracellular edema increased slightly at day 8 to 10 pi, and peaked at day 12 pi. (**E**) Severe edema was evident in all layers at day 14 pi. Note accumulation of mononuclear cells within the vessel (arrows) and enlarged perivascular cells. (**F**) Extracellular edema was still evident at day 28 pi. (**G**) Inoculated control rat showing blood vessel from optic nerve head (arrow). cf (**H**). (**H**) EAE day 14 pi, adhesive leukocytes present within vessel lumens and enlarged perivascular cells. Scale bars, 10 μm; transverse sections stained with toluidine blue.

located predominantly in the peripheral retina, TCR^+ cells were evident mainly in the central region of the retina. Our data indicate that (i) the increase in the number of $ED1^+$ monocytes/macrophages, TCR^+ cells, or MHC class II^+ cells within vessels is apparent 1 day before that in parenchyma; (ii) the time courses for each type of cell, in both vessels and parenchyma, are similar between days 7 and 14 pi; and (iii) unlike TCR^+ and $ED1^+$ cells, MHC class II^+ cells were not detected after day 17 pi.

Discussion

Advantages of the retinal whole-mount technique. In contrast to previous studies that found no evidence of cellular inflammation in the retina of animals with MBP-induced EAE, we have shown that both $ED1^+$ monocytes-macrophages and TCR^+ T cells accumulate in retinal blood vessels and infiltrate the perivascular parenchyma during EAE. This discrepancy is likely attributable to differences in tissue preparation and staining methods. Compared with conventional histological techniques, retinal whole-mounts are more suited for the detection of small numbers of infiltrating cells because they allow visualization of the entire retinal vasculature (Chan-Ling, 1994). The advantages of this system have been demonstrated in studies of the vascular and cellular changes associated with murine cerebral malaria (Chan-Ling *et al*., 1992; Ma *et al*., 1996) and IL-1 induced inflammation (Cuff *et al*., 1996). In addition, unlike the meninges, where wholemounting techniques have also been applied during EAE (Lassmann, 1983), the retinal microvasculature is similar to that of other CNS microvascular plexus in all respects including its embryonic origin, mechanism of formation, astrocytic ensheathment, barrier properties and relationships with pericytes and smooth muscle cells (reviewed in Chan-Ling and Stone, 1993; Chan-Ling, 1994).

Leukocyte trafficking in normal CNS vessels. We have shown that small numbers of leukocytes circulate within the microvasculature of the retina in control animals, likely reflecting leukocyte trafficking through CNS vessels under physiological conditions. However, in only one of six inoculated control rats examined were a small number of $\alpha\beta TCR^+$ cells detected within the tissue parenchyma and this was in marked contrast to the finding in EAE animals.

Breakdown of the BRB is induced by inflammatory cells in the lumen of vessels. Our data confirm previous observations of breakdown of the BRB in EAE (Hayreh, 1981; Sallmann *et al*., 1967). Similar time courses of BRB breakdown were apparent with both HRP and Evans blue as tracers. Tracer leakage into the tissue was first detected 2 to 3 days (days 7 to 8 pi) before significant signs of disease, was maximal (day 14 pi) during overt disease, and was still evident after most signs of disease had disappeared (day 24 pi). Consistent with these observations, perivascular edema was evident in retinal sections during progression of EAE. The time course of breakdown of the BRB was also similar to that of tracer leakage in the brain or spinal cord of rats with acute EAE (Claudio *et al*., 1990; Juhler *et al*., 1984), though the extent was limited compared to tissues containing MBP.

Previous studies have shown that breakdown of the BBB is localized predominantly in blood vessels that exhibit attachment and emigration of inflammatory cells (Claudio *et al*., 1990; Lossinsky *et al*., 1989). Activated T cells have been shown to open the blood-nerve barrier (Pollard *et al*., 1995). We have now provided direct evidence that the disruption of the BRB is colocalized with inflammatory cells present in the vessel lumen. Interleukin-1 and tumor necrosis factor-α are able to initiate many of the changes associated with inflammation of the retinal vasculature (Claudio *et al*., 1994). During the progression of EAE, the activated inflammatory cells release cytokines (Claudio *et al*., 1990), so that the segments of vessels in which inflammatory cells accumulate might be expected to contain high concentrations of these mediators and therefore to exhibit localized changes in permeability. Thus, adhesion of inflammatory cells within a vessel lumen likely plays an important role in dysfunction of the BRB.

Early microglial activation is associated with BRB breakdown. Microglial activation is accompanied by a change in morphology from a ramified to a rod-shaped or rounded appearance, as well as by expression of MHC class II and ED1 antigens (Matsumoto, 1994). In the present study, microglial activation and redistribution towards blood vessels began at day 7 to 8 pi, becoming more marked as the animals developed signs of the disease (days 10 to 12 pi). This is an important finding since microglia and macrophages are major sources of TNFα, which effectively increases BBB permeability (Claudio *et al*., 1994; Spies *et al*., 1995). Earlier workers (Gehrmann *et al*., 1993) have shown that microglial activation in EAE may be induced by direct contact with T cells, thereby facilitating the transfer of mediators such as interleukin-4 and interferon-γ (Mat-

sumoto, 1994) between the cells. However, our observation that microglia activation and breakdown of the BRB occur almost concurrently in acute EAE suggests that inflammatory mediators in the circulatory system can reach microglia as a result of breakdown of the BBB; such a mechanism for induction of microglial activation may predominate in the early stages of EAE.

Intensity of inflammatory response is dependent on encountering significant amounts of the encephalitogenic antigen in the tissue parenchyma. We have provided evidence for a mild perivascular inflammatory response, consisting of breakdown of the BRB, microglial activation and cellular infiltration, in the retina of Lewis rats with EAE. This contrasts greatly with the extent of barrier breakdown and cellular infiltration observed in the myelinated regions of the optic nerve (see preceding manuscript). Notwithstanding the difference in the thickness of the optic nerve section (8μm), compared to the thickness of the retinal wholemount (200-250μm), T cell infiltration at the peak of the inflammatory response observed in the myelinated region of the optic nerve was approximately 570 times that observed in the retina. Similarly, the number of $ED1^+$ cells observed in the parenchyma of the optic nerve was 110 times that observed in the retina. It is likely that this marked difference is due to the amount of MBP (the encephalitogenic antigen used in this study) in the myelinated optic nerve. Our observations on 12 JC Lewis rats using toluidine-blue cross sections showed no evidence of intra-retinal myelination (personal observations).

Earlier studies using bone marrow chimeras (Hinrichs *et al*., 1987; Hickey and Kimura, 1988) have shown that MBP specific cells are recognised by antigen presenting cells in the perivascular and meningeal regions. It is likely that similar perivascular antigen presenting cells are present within the retina and they may contain small amounts of soluble MBP or peptide fragments of MBP liberated from the myelin sheath into the extracellular space of the brain, including the retina. The marked difference in response observed in the retina versus the myelinated region of the optic nerve suggests that only a mild inflammatory response is possible in the absence of substantial quantities of inciting antigen and cells which express MHC class II molecules. Thus, MHC class II expression by resident microglia (parenchymal versus perivascular) may be a possible effective amplifier mechanism, if the encephalitogenic antigen is encountered in the tissue parenchyma (Hickey, 1991; Lassmann *et al*., 1991 and present study).

Acknowledgements

We thank B. Hall and J. Sedgwick for antibodies R73 and OX6; S. Hodgkinson and G. Tran for assistance with induction of experimental animals; J. Sedgwick for helpful discussions during the preparation of this manuscript; C. Jeffrey and R. Smith for assistance with photography; and P. Kent for technical assistance.

This work was supported by grants to T. C.-L and J. P. from the National Multiple Sclerosis Society of Australia and the National Health and Medical Research Council of Australia

References

1. Arnold AC, Pepose JS, Hepler RS, Foos RY (1984) Retinal periphlebitis and retinitis in multiple sclerosis. I. Pathological characteristics. *Ophthalmology* 91: 255-262
2. Chan-Ling T (1994) Glial, neuronal and vascular interaction in the mammalian retina. *Prog Retinal Eye Res* 13: 357-389
3. Chan-Ling T (1997) Glial, vascular, and neuronal cytogenesis in whole-mounted cat retina. *Microsc Res Tech* 36: 1-16
4. Chan-Ling T, Halasz P, Stone J (1990) Development of retinal vasculature in the cat: stages, topography and mechanisms. *Curr Eye Res* 9: 459-478
5. Chan-Ling T, Neill AL, Hunt NH (1992) Early microvascular changes in murine cerebral malaria detected in retina wholemounts. *Am J Pathol* 140: 1121-1130
6. Chan-Ling T, Stone J (1993) Retinopathy of prematurity: origins in the architecture of the retina. . *Prog Retinal Eye Res* 12: 155-177
7. Claudio L, Kress Y, Factor J, Brosnan CF (1990) Mechanisms of edema formation in experimental autoimmune encephalomyelitis. The contribution of inflammatory cells. *Am J Pathol* 137: 1033-1045
8. Claudio L, Martiney JA, Brosnan CF (1994) Ultrastructural studies of the blood-retina barrier after exposure to interleukin-1b or tumor necrosis factor-a. *Lab Invest* 70: 850-861
9. Cuff CA, Berman JW, Brosnan CF (1996) The ordered array of perivascular macrophages is disrupted by IL-1 induced inflammation in the rabbit retina. *Glia* 17: 307-316
10. Engell T, Jensen OA, Klinken L (1985) Periphlebitis retinae in multiple sclerosis. A histopathological study of two cases. *Acta Ophthalmol* 63: 83-88
11. Gehrmann J, Gold R, Linington C, Lannes VJ, Wekerle H, Kreutzberg GW (1993) Microglial involvement in experimental autoimmune inflammation of the central and peripheral nervous system. *Glia* 7: 50-59
12. Hayreh SS (1981) Experimental allergic encephalomyelitis. II. Retinal and other ocular manifestations. *Invest Ophthalmol Vis Sci* 21: 270-281
13. Hickey WF (1991) Migration of hematogenous cells through the blood brain barrier and the initiation of CNS inflammation. *Brain Pathol* 1: 97-106

14. Hickey WF, Kimura H (1988) Perivascular microglial cells of the CNS are bone marrow-derived and present antigen in vivo. *Science* 239: 290-292
15. Hinrichs DJ, Wegmann KW, Dietsch GN (1987) Transfer of EAE to bone marrow chimeras. Endothelial cells are not restricting element. *J Exp Med* 166: 1906-1911
16. Juhler M, Barry DI, Offner H, Konat G, Klinken L, Paulson OB (1984) Blood-brain and blood-spinal cord barrier permeability during the course of experimental allergic encephalomyelitis in the rat. *Brain Res* 302: 347-355
17. Lassmann H (1983) Comparative neuropathology of chronic experimental allergic encephalomyelitis and multiple sclerosis. *New York: Springer*.
18. Lassmann H, Zimprich F, Rossler K, Vass K (1991) Inflammation in the Nervous system: basic mechanisms and immunological concepts. *Rev Neurol* 147: 763-781
19. Lightman S, McDonald WI, Bird AC, Francis DA, Hoskins A, Batchelor JR, Halliday AM (1987) Retinal venous sheathing in optic neuritis. Its significance for the pathogenesis of multiple sclerosis. *Brain* 110: 405-414
20. Lossinsky AS, Badmajew V, Robson JA, Moretz RC, Wisniewski HM (1989) Sites of egress of inflammatory cells and horseradish peroxidase transport across the blood-brain barrier in a murine model of chronic relapsing experimental allergic encephalomyelitis. *Acta Neuropathol* 78: 359-371
21. Ma N, Hunt NH, Madigan MC, Chan-Ling T (1996) Correlation between enhanced vascular permeability, up-regulation of cellular adhesion molecules and monocyte adhesion to the endothelium in the retina during the development of fatal murine cerebral malaria. *Am J Pathol* 149: 1745-1761
22. Matsumoto Y (1994) Role of microglia in autoimmune encephalomyelitis. *Neuropath Appl Neuro* 20: 196-198
23. Pollard JD, Westland KW, Harvey GK, Jung S, Bonner J, Spies JM, Toyka KV, Hartung HP (1995) Activated T cells of nonneural specificity open the blood-nerve barrier to circulating antibody. *Ann Neurol* 37: 467-475
24. Rao NA, Tso MO, Zimmerman EL (1977) Experimental allergic optic neuritis in guinea pigs: preliminary report. *Invest Ophthalmol Vis Sci* 16: 338-342
25. Sallmann LV, Myers RE, Lerner EM, Stone SH (1967) Vasculo-occlusive retinopathy in experimental allergic encephalomyelitis. *Arch Ophthalmol* 78: 112-120
26. Shikishima K, Lee WR, Behan WM, Foulds WS (1993) Uveitis and retinal vasculitis in acute experimental allergic encephalomyelitis in the Lewis rats: an ultrastructural study. *Exp Eye Res* 56: 167-175
27. Spies JM, Westland KW, Bonner JG, Pollard JD (1995) Intraneural activated T cells cause focal breakdown of the blood-nerve barrier. *Brain* 118: 857-68
28. Verhagen C, Mor F, Cohen IR (1994) T cell immunity to myelin basic protein induces anterior uveitis in Lewis rats. *J Neuroimmunol* 53: 65-71
29. Wekerle H (1993) T-cell autoimmunity in the central nervous system. *Intervirology* 35: 95-100
30. Wray SH (1997) Optic Neuritis In: Multiple sclerosis: Clinical and pathogenetic basis. Raine CS, McFarland HF, Tourtellotte WW (eds), Chapter 2, pp. 21-30, Chapman & Hall Medical: London, Weinheim, New York, Tokyo, Melbourne, Madras